

# Muon capture on deuteron and $^3\text{He}$

L.E. Marcucci<sup>1,2</sup>, M. Piarulli<sup>3</sup>, M. Viviani<sup>2</sup>, L. Girlanda<sup>1,2</sup>, A. Kievsky<sup>2</sup>, S. Rosati<sup>1,2</sup>, and R. Schiavilla<sup>3,4</sup>

<sup>1</sup> *Department of Physics, University of Pisa, 56127, Pisa, Italy*

<sup>2</sup> *INFN-Pisa, 56127, Pisa, Italy*

<sup>3</sup> *Department of Physics, Old Dominion University, Norfolk, VA 23529, USA*

<sup>4</sup> *Jefferson Lab, Newport News, VA 23606, USA*

The muon capture reactions  $^2\text{H}(\mu^-, \nu_\mu)nn$  and  $^3\text{He}(\mu^-, \nu_\mu)^3\text{H}$  are studied with conventional or chiral realistic potentials and consistent weak currents. The initial and final  $A = 2$  and  $3$  nuclear wave functions are obtained from the Argonne  $v_{18}$  or chiral N3LO two-nucleon potential, in combination with, respectively, the Urbana IX or chiral N2LO three-nucleon potential in the case of  $A = 3$ . The weak current consists of polar- and axial-vector components. The former are related to the isovector piece of the electromagnetic current via the conserved-vector-current hypothesis. These and the axial currents are derived either in a meson-exchange or in a chiral effective field theory ( $\chi\text{EFT}$ ) framework. There is one parameter (either the  $N$ -to- $\Delta$  axial coupling constant in the meson-exchange model, or the strength of a contact term in the  $\chi\text{EFT}$  model) which is fixed by reproducing the Gamow-Teller matrix element in tritium  $\beta$ -decay. The model dependence relative to the adopted interactions and currents (and cutoff sensitivity in the  $\chi\text{EFT}$  currents) is weak, resulting in total rates of  $392.0 \pm 2.3 \text{ s}^{-1}$  for  $A = 2$ , and  $1484 \pm 13 \text{ s}^{-1}$  for  $A = 3$ , where the spread accounts for this model dependence.

PACS numbers: 23.40.-s, 21.45.-v, 27.10.+h

## I. INTRODUCTION

There is a significant body of experimental and theoretical work on muon capture in nuclei (see Refs. [1, 2] for a review). These processes provide a testing ground for wave functions and, indirectly, the interactions from which these are obtained, and for models of the nuclear weak current. This is particularly important for neutrino reactions in light nuclei [3] and for processes, such as the astrophysically relevant weak captures on proton and  $^3\text{He}$ , whose rates cannot be measured experimentally, and for which one has to rely exclusively on theory. Thus, it becomes crucial to study within the same theoretical framework related electroweak transitions, whose rates are known experimentally [4]. Muon captures are among such reactions.

In the present work, we focus our attention on muon capture on deuteron and  $^3\text{He}$ , i.e., on the reactions

$$\mu^- + d \rightarrow n + n + \nu_\mu, \quad (1.1)$$

$$\mu^- + ^3\text{He} \rightarrow ^3\text{H} + \nu_\mu. \quad (1.2)$$

Muon capture on  $^3\text{He}$  can also occur through the two- ( $nd$ ) and three-body ( $nnp$ ) breakup channels of  $^3\text{H}$ . However, the branching ratios of these two processes are 20% and 10%, respectively, and will not be considered in the present work.

These reactions have been studied extensively through the years, experimentally and theoretically. In reaction (1.1), the stopped muons are captured from two hyperfine states,  $f = 1/2$  or  $3/2$ . The doublet capture rate  $\Gamma^D$  has been calculated by several groups to be about 40 times larger than the quadruplet [1, 2]. We will therefore consider only  $\Gamma^D$ . The first attempt to measure  $\Gamma^D$  was

carried out over forty years ago by Wang *et al.*: they obtained  $\Gamma^D = 365(96) \text{ s}^{-1}$  [5]. A few years later, Bertin *et al.* measured  $\Gamma^D = 445(60) \text{ s}^{-1}$  [6]. Measurements performed in the eighties gave  $\Gamma^D = 470(29) \text{ s}^{-1}$  [7] and  $\Gamma^D = 409(40) \text{ s}^{-1}$  [8]. These measurements, while consistent with each other, are not very precise – errors are in the 6–10 % range. However, there is hope to have this situation clarified by the MuSun Collaboration [9], which is expected to perform an experiment at the Paul Scherrer Institut, with the goal of measuring  $\Gamma^D$  with a precision of 1 %.

The experimental situation for reaction (1.2) is much clearer: after a first set of measurements in the early sixties [10–13], a very precise determination in the late nineties yielded a total capture rate  $\Gamma_0 = 1496(4) \text{ s}^{-1}$  [14], a value consistent with those of the earlier measurements, although these were affected by considerably larger uncertainties.

Theoretical work on reactions (1.1) and (1.2) is just as extensive, and a list of publications, updated to the late nineties, is given in Table 4.1 of Ref. [1], and in Ref. [2]. Here, we limit our considerations to the calculations of Refs. [15–17]. We also comment on the recent studies of Ando *et al.* [18] and Ricci *et al.* [19].

The calculations of Refs. [15–17] were performed within the “Standard Nuclear Physics Approach” (SNPA): their authors used the realistic potential models available at the time to obtain the nuclear wave functions, and included in the nuclear weak current operator one-body (impulse approximation) and two-body operators. In Ref. [15],  $\Gamma^D$  was calculated to be  $416(7) \text{ s}^{-1}$ , the uncertainty coming from imprecise knowledge of the coupling constants, and in Refs. [16] and [17]  $399 \text{ s}^{-1}$  and  $402 \text{ s}^{-1}$ , respectively. The results of Refs. [16] and [17] are in

good agreement with each other, while that of Ref. [15] differs by  $\sim 4\%$ . It is important to note, however, that the meson-exchange currents (MEC) contributions were not constrained to reproduce any experimental observable, such as the triton half-life, as is now common practice [20–22].

Reference [18] overcame some of the limitations inherent to the earlier studies. Much along the lines of Ref. [22], reaction (1.1) was studied within a hybrid chiral effective field theory ( $\chi$ EFT) approach, in which matrix elements of weak operators derived in  $\chi$ EFT were evaluated between wave functions obtained from a realistic potential, specifically the Argonne  $v_{18}$  (AV18) [23]. The  $\chi$ EFT axial current contains a low-energy constant which was fixed by reproducing the experimental Gamow-Teller matrix element ( $GT^{\text{EXP}}$ ) in tritium  $\beta$ -decay. The calculation, however, retained only the  $S$ -wave contribution in the  $nn$  final scattering state (the  $^1S_0$  state), and higher partial-wave contributions were taken from Ref. [16]. This approach yielded a value for  $\Gamma^D$  of  $386\text{ s}^{-1}$ , with  $\Gamma^D(^1S_0)=245(1)\text{ s}^{-1}$ , the theoretical error being related to the experimental uncertainty in  $GT^{\text{EXP}}$ .

The latest SNPA calculation of muon capture on deuteron has been carried out in Ref. [19], and has led to values in the range of  $416\text{--}430\text{ s}^{-1}$  (see Table 1 of Ref. [19]), depending on the potential used, the Nijmegen I or Nijmegen 93 [24]. However, the model for the axial current is not constrained by data, resulting in the relatively large spread in  $\Gamma^D$  values.

Finally, there is a calculation based on pionless EFT [25] with the objective of constraining the two-nucleon axial current matrix element by reproducing the muon capture rate on deuterons. This same matrix element enters the  $pp$  weak capture.

Theoretical studies for reaction (1.2) within the SNPA have been performed in the early nineties by Congleton and Fearing [26] and Congleton and Truhlik [27]. In this later work, the nuclear wave functions were obtained from a realistic Hamiltonian based on the Argonne  $v_{14}$  (AV14) two-nucleon [28] and the Tucson-Melbourne (TM) three-nucleon [29] interactions. The nuclear weak current retained contributions similar to those of Ref. [19]. The value obtained for the total capture rate  $\Gamma_0$  was  $1502(32)\text{ s}^{-1}$ , the uncertainty due to poor knowledge of some of the coupling constants and cutoff parameters entering the axial current.

A first study of the model-dependence of predictions for the total rate of muon capture on  $^3\text{He}$  was carried out in Ref. [30], within the SNPA, but without the inclusion of MEC contributions. Values for  $\Gamma_0$  were found to vary by  $\simeq 100\text{ s}^{-1}$ , depending on the potential model considered. Both old- (Paris [31], Bonn A and B [32], AV14) and new-generation (Nijmegen I [24] and CD-Bonn [33]) potentials were used. However, no three-nucleon forces were included. This second aspect of the calculation, along with the absence of MEC contributions, might be the origin of the large model dependence observed in the results.

A first attempt to study muon capture on  $^3\text{He}$  in a way that was consistent with the approach adopted for the weak proton capture reactions, involved some of the present authors [34]. The nuclear wave functions were obtained with the hyperspherical-harmonics (HH) method (see Ref. [35] for a recent review), from a realistic Hamiltonian based on the AV18 two-nucleon and Urbana IX [36] (UIX) three-nucleon interactions. The model for the nuclear weak current was taken from Refs. [20, 21]. However, two additional contributions were included: the single-nucleon pseudoscalar charge operator and the pseudoscalar two-body term in the  $N$ -to- $\Delta$  transition axial current. Both contributions are of order  $O(q^2/m^2)$ , where  $q$  is the momentum transfer in the process and  $m$  is the nucleon mass, and were obviously neglected in the  $pp$  and  $hep$  captures of Refs. [20, 21], for which  $q \ll m$ . The axial coupling constant for the  $N$ -to- $\Delta$  transition was constrained to reproduce  $GT^{\text{EXP}}$ . The total capture rate  $\Gamma_0$  was found to be  $1484(8)\text{ s}^{-1}$ , where the uncertainty results from the adopted fitting procedure and experimental error on  $GT^{\text{EXP}}$ . A calculation based on the older AV14/TM Hamiltonian model yielded a  $\Gamma_0$  of  $1486(8)\text{ s}^{-1}$ , suggesting a weak model-dependence.

Recently, a hybrid calculation has appeared [37], in which the nuclear wave functions have been obtained with the Effective Interaction HH method [38], and the  $\chi$ EFT weak current is that of Ref. [22]. It has yielded a value for  $\Gamma_0$  of  $1499(16)\text{ s}^{-1}$ , where the error has two main sources: the experimental uncertainty on the triton half-life, and the calculation of radiative corrections.

In light of the previous considerations, it is clear that a calculation is still lacking which: (i) treats reactions (1.1) and (1.2) simultaneously in a consistent framework, either SNPA or  $\chi$ EFT; (ii) is based on up-to-date Hamiltonian models to generate the wave functions; (iii) reduces the model dependence of the weak axial current by constraining it to reproduce  $GT^{\text{EXP}}$ . The goal of the present work is to fill this gap. The calculation has been structured as follows: the nuclear Hamiltonian models considered consist of the AV18 and N3LO [39] two-nucleon interactions for the  $A = 2$  systems, augmented by the UIX and N2LO [40] three-nucleon interactions for the  $A = 3$  systems. The nuclear weak current is derived from either SNPA or  $\chi$ EFT. In both cases, its axial component is calibrated by fitting  $GT^{\text{EXP}}$ , while its vector part is related to the isovector electromagnetic current by the conserved-vector-current (CVC) hypothesis. The SNPA version of it reproduces well static magnetic properties of few-nucleons systems. In the  $\chi$ EFT electromagnetic current of Ref. [42], adopted in the present work, the two low-energy constants are fixed by reproducing the trinucleon magnetic moments.

In closing, we note that the study of Ref. [34] has established that the total rate of reaction (1.2) scales approximately linearly with the trinucleon binding energy. Thus a realistic calculation of this rate must, at a minimum, include a three-nucleon potential which reproduces well these energies (as is the case here). Finally,

we could have adopted the set of two-nucleon chiral potentials at N3LO derived by the Bonn group [41] for a range of cutoff parameters  $\Lambda$ , in order to explore the sensitivity of the results to the short-range behavior of the potentials. However, the potentials considered in the present study (AV18 and N3LO) have so drastically different treatments of this short-range behavior that they should provide a meaningful measure of the model dependence originating from it.

The paper is organized as follows. In Sec. II we list the explicit expressions for the observables of interest in terms of reduced matrix elements of multipole operators. In the case of reaction (1.2) the derivation is given in Ref. [34]. In Sec. III, we briefly review the method used to calculate the nuclear wave functions and summarize the main results for the observables of the nuclear systems involved in the reactions of interest. In Sec. IV, we describe the model for the nuclear weak current, both its SNPA and  $\chi$ EFT versions. In Sec. V, we present and discuss the results obtained for the total capture rates of reactions (1.1) and (1.2), and finally in Sec. VI we summarize our conclusions.

## II. OBSERVABLES

The muon capture on deuteron and  $^3\text{He}$  is induced by the weak interaction Hamiltonian [43]

$$H_W = \frac{G_V}{\sqrt{2}} \int d\mathbf{x} l_\sigma(\mathbf{x}) j^\sigma(\mathbf{x}) , \quad (2.1)$$

where  $G_V$  is the Fermi coupling constant,  $G_V = 1.14939 \times 10^{-5} \text{ GeV}^{-2}$  as obtained from an analysis of  $0^+$  to  $0^+$

$\beta$ -decays [44], and  $l_\sigma$  and  $j^\sigma$  are the leptonic and hadronic current densities, respectively. The former is given by

$$l_\sigma(\mathbf{x}) = e^{-i\mathbf{k}_\nu \cdot \mathbf{x}} \bar{u}(\mathbf{k}_\nu, h_\nu) \gamma_\sigma (1 - \gamma_5) \psi_\mu(\mathbf{x}, s_\mu) , \quad (2.2)$$

where  $\psi_\mu(\mathbf{x}, s_\mu)$  is the ground-state wave function of the muon in the Coulomb field of the nucleus in the initial state, and  $u(\mathbf{k}_\nu, h_\nu)$  is the spinor of a muon neutrino with momentum  $\mathbf{k}_\nu$ , energy  $E_\nu (=k_\nu)$ , and helicity  $h_\nu$ . While in principle the relativistic solution of the Dirac equation could be used, in practice it suffices to approximate

$$\begin{aligned} \psi_\mu(\mathbf{x}, s_\mu) &\simeq \psi_{1s}(x) \chi(s_\mu) \equiv \psi_{1s}(x) u(\mathbf{k}_\mu, s_\mu) \\ \mathbf{k}_\mu &\rightarrow 0 , \end{aligned} \quad (2.3)$$

since the muon velocity  $v_\mu \simeq Z\alpha \ll 1$  ( $\alpha$  is the fine-structure constant and  $Z=1$  or  $2$  for deuteron or  $^3\text{He}$ , respectively). Here  $\psi_{1s}(x)$  is the  $1s$  solution of the Schrödinger equation and, since the muon is essentially at rest, it is justified to replace the two-component spin state  $\chi(s_\mu)$  with the four-component spinor  $u(\mathbf{k}_\mu, s_\mu)$  in the limit  $\mathbf{k}_\mu \rightarrow 0$ . This will allow us to use standard techniques to carry out the spin sum over  $s_\mu$  at a later stage.

In order to account for the hyperfine structure in the initial system, the muon and deuteron or  $^3\text{He}$  spins are coupled to states with total spin  $f$ , equal to  $1/2$  or  $3/2$  in the deuteron case, and to  $0$  or  $1$  in the  $^3\text{He}$  case. The transition amplitude can then be conveniently written as

$$\begin{aligned} T_W(f, f_z; s_1, s_2, h_\nu) &\equiv \langle nn, s_1, s_2; \nu, h_\nu | H_W | (\mu, d); f, f_z \rangle \\ &\simeq \frac{G_V}{\sqrt{2}} \psi_{1s}^{\text{av}} \sum_{s_\mu s_d} \langle \frac{1}{2} s_\mu, 1 s_d | f f_z \rangle l_\sigma(h_\nu, s_\mu) \langle \Psi_{\mathbf{p}, s_1 s_2}(nn) | j^\sigma(\mathbf{q}) | \Psi_d(s_d) \rangle , \end{aligned} \quad (2.4)$$

for the muon capture on deuteron, where  $\mathbf{p}$  is the  $nn$

relative momentum, and [34]

$$\begin{aligned} T_W(f, f_z; s'_3, h_\nu) &\equiv \langle ^3\text{H}, s'_3; \nu, h_\nu | H_W | (\mu, ^3\text{He}); f, f_z \rangle \\ &\simeq \frac{G_V}{\sqrt{2}} \psi_{1s}^{\text{av}} \sum_{s_\mu s_3} \langle \frac{1}{2} s_\mu, \frac{1}{2} s_3 | f f_z \rangle l_\sigma(h_\nu, s_\mu) \langle \Psi_{^3\text{H}}(s'_3) | j^\sigma(\mathbf{q}) | \Psi_{^3\text{He}}(s_3) \rangle , \end{aligned} \quad (2.5)$$

for muon capture on  $^3\text{He}$ . In Eqs. (2.4) and (2.5) we have

defined

$$l_\sigma(h_\nu, s_\mu) \equiv \bar{u}(\mathbf{k}_\nu, h_\nu) \gamma_\sigma (1 - \gamma_5) u(\mathbf{k}_\mu, s_\mu) , \quad (2.6)$$

and the Fourier transform of the nuclear weak current has been introduced as

$$j^\sigma(\mathbf{q}) = \int d\mathbf{x} e^{i\mathbf{q}\cdot\mathbf{x}} j^\sigma(\mathbf{x}) \equiv (\rho(\mathbf{q}), \mathbf{j}(\mathbf{q})) \quad , \quad (2.7)$$

with the leptonic momentum transfer  $\mathbf{q}$  defined as  $\mathbf{q} = \mathbf{k}_\mu - \mathbf{k}_\nu \simeq -\mathbf{k}_\nu$ . The function  $\psi_{1s}(x)$  has been factored out from the matrix element of  $j^\sigma(\mathbf{q})$  between the initial and final states. For muon capture on deuteron,  $\psi_{1s}^{\text{av}}$  is approximated as [43]

$$|\psi_{1s}^{\text{av}}|^2 \equiv |\psi_{1s}(0)|^2 = \frac{(\alpha \mu_{\mu d})^3}{\pi} \quad , \quad (2.8)$$

where  $\psi_{1s}(0)$  denotes the Bohr wave function for a point charge  $e$  evaluated at the origin, and  $\mu_{\mu d}$  is the reduced mass of the  $(\mu, d)$  system. For muon capture on  $^3\text{He}$ ,  $\psi_{1s}^{\text{av}}$  is approximated as [34]

$$|\psi_{1s}^{\text{av}}|^2 \equiv \mathcal{R} \frac{(2\alpha \mu_{\mu^3\text{He}})^3}{\pi} \quad , \quad (2.9)$$

where in this case  $\mu_{\mu^3\text{He}}$  is the reduced mass of the  $(\mu, ^3\text{He})$  system, and the factor  $\mathcal{R}$  approximately ac-

counts for the finite extent of the nuclear charge distribution [43]. This factor is defined as

$$\mathcal{R} = \frac{|\psi_{1s}^{\text{av}}|^2}{|\psi_{1s}(0)|^2} \quad , \quad (2.10)$$

with

$$\psi_{1s}^{\text{av}} = \frac{\int d\mathbf{x} e^{i\mathbf{q}\cdot\mathbf{x}} \psi_{1s}(x) \rho(x)}{\int d\mathbf{x} e^{i\mathbf{q}\cdot\mathbf{x}} \rho(x)} \quad , \quad (2.11)$$

where  $\rho(x)$  is the  $^3\text{He}$  charge density. It has been calculated explicitly by using the charge densities corresponding to the two Hamiltonian models considered in the present study (AV18/UIX and N3LO/N2LO), and has been found to be, for both models, within a percent of 0.98, the value commonly adopted in the literature [43].

In the case of muon capture on deuteron, the final state wave function is expanded in partial waves as

$$\Psi_{\mathbf{p}, s_1, s_2}(nn) = 4\pi \sum_S \langle \frac{1}{2} s_1, \frac{1}{2} s_2 | SS_z \rangle \sum_{LJJ_z} i^L Y_{LL_z}^*(\hat{\mathbf{p}}) \langle SS_z, LL_z | JJ_z \rangle \overline{\Psi}_{nn}^{LSJJ_z}(p) \quad , \quad (2.12)$$

where  $\overline{\Psi}_{nn}^{LSJJ_z}(p)$  is the  $nn$  wave function – it will be discussed in Sec. III. In the present work, we restrict our calculation to  $J \leq 2$  and  $L \leq 3$ , and therefore the contributing partial waves are, in a spectroscopic notation,  $^1S_0$ ,  $^3P_0$ ,  $^3P_1$ ,  $^3P_2$ – $^3F_2$  and  $^1D_2$ .

Standard techniques [21, 43] are now used to carry out the multipole expansion of the weak charge,  $\rho(\mathbf{q})$ , and current,  $\mathbf{j}(\mathbf{q})$ , operators. For muon capture on deuteron, we find

$$\langle \overline{\Psi}_{nn}^{LSJJ_z}(p) | \rho(\mathbf{q}) | \Psi_d(s_d) \rangle = \sqrt{4\pi} \sum_{\Lambda \geq 0} \sqrt{2\Lambda+1} i^\Lambda \frac{\langle 1s_d, \Lambda 0 | JJ_z \rangle}{\sqrt{2J+1}} C_\Lambda^{LSJ}(q) \quad , \quad (2.13)$$

$$\langle \overline{\Psi}_{nn}^{LSJJ_z}(p) | j_z(\mathbf{q}) | \Psi_d(s_d) \rangle = -\sqrt{4\pi} \sum_{\Lambda \geq 0} \sqrt{2\Lambda+1} i^\Lambda \frac{\langle 1s_d, \Lambda 0 | JJ_z \rangle}{\sqrt{2J+1}} L_\Lambda^{LSJ}(q) \quad , \quad (2.14)$$

$$\langle \overline{\Psi}_{nn}^{LSJJ_z}(p) | j_\lambda(\mathbf{q}) | \Psi_d(s_d) \rangle = \sqrt{2\pi} \sum_{\Lambda \geq 1} \sqrt{2\Lambda+1} i^\Lambda \frac{\langle 1s_d, \Lambda - \lambda | JJ_z \rangle}{\sqrt{2J+1}} [-\lambda M_\Lambda^{LSJ}(q) + E_\Lambda^{LSJ}(q)] \quad , \quad (2.15)$$

where  $\lambda = \pm 1$ , and  $C_\Lambda^{LSJ}(q)$ ,  $L_\Lambda^{LSJ}(q)$ ,  $E_\Lambda^{LSJ}(q)$  and  $M_\Lambda^{LSJ}(q)$  denote the reduced matrix elements (RMEs) of the Coulomb ( $C$ ), longitudinal ( $L$ ), transverse electric ( $E$ ) and transverse magnetic ( $M$ ) multipole operators, as defined in Ref. [21]. Since the weak charge and cur-

rent operators have scalar/polar-vector ( $V$ ) and pseudo-scalar/axial-vector ( $A$ ) components, each multipole consists of the sum of  $V$  and  $A$  terms, having opposite parity under space inversions [21]. The contributing multipoles for the  $S$ -,  $P$ -, and  $D$ -channels considered in the present

work are listed in Table I, where the superscripts  $LSJ$  have been dropped.

In the case of muon capture on  $^3\text{He}$ , explicit expressions for the multipole operators can be found in Ref. [34]. Here we only note that parity and angular momentum selection rules restrict the contributing RMEs to  $C_0(V)$ ,  $C_1(A)$ ,  $L_0(V)$ ,  $L_1(A)$ ,  $E_1(A)$ , and  $M_1(V)$ .

The total capture rate for the two reactions under consideration is then defined as

$$d\Gamma = 2\pi\delta(\Delta E)|\overline{T_W}|^2 \times (\text{phase space}) , \quad (2.16)$$

where  $\delta(\Delta E)$  is the energy-conserving  $\delta$ -function, and the phase space is  $d\mathbf{p} d\mathbf{k}_\nu / (2\pi)^6$  for reaction (1.1) and just  $d\mathbf{k}_\nu / (2\pi)^3$  for reaction (1.2). The following notation has been introduced: (i) for muon capture on deuteron

$$|\overline{T_W}|^2 = \frac{1}{2f+1} \sum_{s_1 s_2 h_\nu} \sum_{f_z} |T_W(f, f_z; s_1, s_2, h_\nu)|^2 , \quad (2.17)$$

and the initial hyperfine state has been fixed to be  $f = 1/2$ ; (ii) for muon capture on  $^3\text{He}$

$$|\overline{T_W}|^2 = \frac{1}{4} \sum_{s'_3 h_\nu} \sum_{ff_z} |T_W(f, f_z; s'_3, h_\nu)|^2 , \quad (2.18)$$

and the factor 1/4 follows from assigning the same probability to all different hyperfine states.

After carrying out the spin sums, the total rate for muon capture on  $^3\text{He}$  reads [34]

$$\Gamma_0 = G_V^2 E_\nu^2 \left(1 - \frac{E_\nu}{m_{^3\text{H}}}\right) |\psi_{1s}^{\text{av}}|^2 \left[ |C_0(V) - L_0(V)|^2 + |C_1(A) - L_1(A)|^2 + |M_1(V) - E_1(A)|^2 \right] , \quad (2.19)$$

with  $E_\nu$  given by

$$E_\nu = \frac{(m_\mu + m_{^3\text{He}})^2 - m_{^3\text{H}}^2}{2(m_\mu + m_{^3\text{He}})} . \quad (2.20)$$

In the case of muon capture on deuteron, the differential rate reads

$$\frac{d\Gamma_D}{dp} = E_\nu^2 \left[1 - \frac{E_\nu}{(m_\mu + m_d)}\right] |\psi_{1s}^{\text{av}}|^2 \frac{p^2 d\mathbf{p}}{8\pi^4} |\overline{T_W}|^2 , \quad (2.21)$$

where

$$E_\nu = \frac{(m_\mu + m_d)^2 - 4m_n^2 - 4p^2}{2(m_\mu + m_d)} . \quad (2.22)$$

In Eqs. (2.19)–(2.22),  $m_\mu$ ,  $m_n$ ,  $m_d$ ,  $m_{^3\text{H}}$ ,  $m_{^3\text{He}}$  are the muon, neutron, deuteron,  $^3\text{H}$  and  $^3\text{He}$  masses. The integration over  $\mathbf{p}$  in Eq. (2.21) is performed numerically using Gauss-Legendre points, and a limited number of them, of the order of 10, is necessary to achieve convergence to better than 1 part in  $10^3$ . In order to calculate the total capture rate  $\Gamma^D$ , the differential capture rate is plotted versus  $p$ , and numerically integrated. Usually, about 30 points in  $p$  are enough for this integration in each partial wave. The differential cross section for each contributing partial wave will be shown in Sec. V.

### III. NUCLEAR WAVE FUNCTIONS

Bound and continuum wave functions for both two- and three-nucleon systems are obtained with the hyperspherical-harmonics (HH) expansion method. This method, as implemented in the case of  $A = 3$  systems, has been reviewed in considerable detail in a series of recent publications [35, 45, 46]. We will discuss it here in the context of  $A = 2$  systems, for which, of course, wave

Partial wave	Contributing multipoles
$^1S_0$	$C_1(A), L_1(A), E_1(A), M_1(V)$
$^3P_0$	$C_1(V), L_1(V), E_1(V), M_1(A)$
$^3P_1$	$C_0(A), L_0(A),$ $C_1(V), L_1(V), E_1(V), M_1(A),$ $C_2(A), L_2(A), E_2(A), M_2(V)$
$^3P_2$ – $^3F_2$	$C_1(V), L_1(V), E_1(V), M_1(A),$ $C_2(A), L_2(A), E_2(A), M_2(V),$ $C_3(V), L_3(V), E_3(V), M_3(A)$
$^1D_2$	$C_1(A), L_1(A), E_1(A), M_1(V),$ $C_2(V), L_2(V), E_2(V), M_2(A),$ $C_3(A), L_3(A), E_3(A), M_3(V)$

TABLE I: Contributing multipoles in muon capture on deuteron, for all the  $nn$  partial waves with  $J \leq 2$  and  $L \leq 3$ . The spectroscopic notation is used. See text for further explanations.

functions could have been obtained by direct solution of the Schrödinger equation.

The nuclear wave function for a bound system of total angular momentum  $JJ_z$  can be generally written as

$$|\Psi^{JJ_z}\rangle = \sum_{\mu} c_{\mu} |\Psi_{\mu}^{JJ_z}\rangle, \quad (3.1)$$

where  $|\Psi_{\mu}^{JJ_z}\rangle$  is a complete set of states, and  $\mu$  is an index denoting the set of quantum numbers necessary to completely specify the basis elements. The coefficients of the expansion can be calculated by using the Rayleigh-Ritz variational principle, which states that

$$\langle \delta_c \Psi^{JJ_z} | H - E | \Psi^{JJ_z} \rangle = 0, \quad (3.2)$$

where  $\delta_c \Psi^{JJ_z}$  indicates the variation of  $\Psi^{JJ_z}$  for arbitrary infinitesimal changes of the linear coefficients  $c_{\mu}$ . The problem of determining  $c_{\mu}$  and the energy  $E$  is then reduced to a generalized eigenvalue problem,

$$\sum_{\mu'} \langle \Psi_{\mu}^{JJ_z} | H - E | \Psi_{\mu'}^{JJ_z} \rangle c_{\mu'} = 0. \quad (3.3)$$

In the case of the deuteron, we first define

$$\psi_{LSJJ_z}(\mathbf{r}) = F_{LSJ}(r) \mathcal{Y}_{LSJJ_z}(\hat{\mathbf{r}}), \quad (3.4)$$

where

$$\mathcal{Y}_{LSJJ_z}(\hat{\mathbf{r}}) = [Y_L(\hat{\mathbf{r}}) \otimes \chi_S]_{JJ_z}, \quad (3.5)$$

and  $\mathbf{r}$  is the relative position vector of the two nucleons. Obviously, for the deuteron,  $L = 0$  or  $2$ ,  $S = 1$ ,  $J = 1$ , and  $T = 0$  (the isospin state  $\eta_{TT_z}$  with  $T = T_z = 0$  has been dropped for brevity). The radial functions  $F_{LSJ}(r)$  are then conveniently expanded on a basis of Laguerre polynomials as

$$F_{LSJ}(r) = \sum_l c_{LSJ,l} f_l(r), \quad (3.6)$$

with

$$f_l(r) = \sqrt{\frac{l!}{(l+2)!}} \gamma^{3/2} L_l^{(2)}(\gamma r) e^{-\gamma r/2}, \quad (3.7)$$

where the parameter  $\gamma$  is variationally optimized ( $\gamma$  is in the range of  $3\text{--}4 \text{ fm}^{-1}$  for the AV18 and N3LO potentials). The complete wave function is then reconstructed as

$$\begin{aligned} \Psi^{1J_z} &= \sum_{L=0,2} \sum_l c_{L11,l} f_l(r) \mathcal{Y}_{L11J_z}(\hat{\mathbf{r}}) \\ &\equiv \sum_{\mu} c_{\mu} \Psi_{\mu}^{1J_z}, \end{aligned} \quad (3.8)$$

and the subscript  $\mu$  denotes the set of quantum numbers  $[L, S = 1, J = 1, l]$ .

The  $nn$  continuum wave function is written as

$$\Psi^{LSJJ_z} = \Psi_C^{LSJJ_z} + \Psi_A^{LSJJ_z}, \quad (3.9)$$

where  $\Psi_C^{LSJJ_z}$  describes the system in the region where the two neutrons are close to each other and their mutual interactions are strong, while  $\Psi_A^{LSJJ_z}$  describes their relative motion in the asymptotic region. The function  $\Psi_C^{LSJJ_z}$ , which vanishes in the limit of large separations, is expanded on Laguerre polynomials as before for the case of the deuteron, see Eq. (3.1), while the function  $\Psi_A^{LSJJ_z}$  is the appropriate asymptotic solution in channel  $LSJ$ ,

$$\Psi_A^{LSJJ_z} = \sum_{L'S'} \left[ \delta_{LL'} \delta_{SS'} \Omega_{L'S'JJ_z}^R + \mathcal{R}_{LS,L'S'}^J(p) \Omega_{L'S'JJ_z}^I \right], \quad (3.10)$$

where

$$\Omega_{LSJJ_z}^{R/I} = R_L^{R/I}(pr) \mathcal{Y}_{LSJJ_z}(\hat{\mathbf{r}}), \quad (3.11)$$

with

$$\begin{aligned} R_L^R(pr) &\equiv \frac{1}{pL} j_L(pr), \\ R_L^I(pr) &\equiv p^{L+1} f_R(r) n_L(pr), \end{aligned} \quad (3.12)$$

$p$  being the magnitude of the relative momentum. The functions  $j_L(pr)$  and  $n_L(pr)$  are the regular and irregular spherical Bessel functions, and  $f_R(r) = [1 - \exp(-br)]^{2L+1}$  has been introduced to regularize  $n_L(pr)$  at small values of  $r$ . The trial parameter  $b$  is taken as  $b = 0.25 \text{ fm}^{-1}$ .

The matrix elements  $\mathcal{R}_{LS,L'S'}^J(p)$  and the coefficients  $c_{\mu}$  entering the expansion of  $\Psi_C^{LSJJ_z}$  are determined applying the Kohn variational principle [47], stating that the functional

$$\begin{aligned} [\mathcal{R}_{LS,L'S'}^J(p)] &= \mathcal{R}_{LS,L'S'}^J(p) \\ &- \frac{2\mu}{\hbar^2} \left\langle \Psi^{L'S'JJ_z} \left| H - \frac{p^2}{2\mu} \right| \Psi^{LSJJ_z} \right\rangle, \end{aligned} \quad (3.13)$$

is stationary with respect to variations of the trial parameters in  $\Psi^{LSJJ_z}$ . Here  $\mu$  is the reduced mass of the  $nn$  system. Performing the variation, a system of linear inhomogeneous equations for  $c_{\mu}$  and a set of algebraic equations for  $\mathcal{R}_{LS,L'S'}^J(p)$  are derived, and solved by standard techniques. From the  $\mathcal{R}_{LS,L'S'}^J(p)$ 's, phase shifts, mixing angles, and scattering lengths are easily obtained.

We list in Tables II and III binding energies and scattering lengths calculated with the Hamiltonian models considered in the present work. Note that  $A = 3$  wave functions retain both  $T = 1/2$  and  $T = 3/2$  contributions,  $T$  being the total isospin quantum number. The experimental data are, in general, quite well reproduced. It should be noted that, by using only two-nucleon interaction, the triton and  $^3\text{He}$  binding energies are 7.624 MeV and 6.925 MeV with the AV18, and 7.854 MeV and 7.128 MeV with the N3LO, respectively.

	AV18	N3LO	Exp.
$B_d$ (MeV)	2.22457	2.22456	2.224574(9)
$P_D$ (%)	5.76	4.51	–
$a_{nn}$ (fm)	–18.487	–18.900	–18.9(4)
$^1a_{np}$ (fm)	–23.732	–23.732	–23.740(20)
$^3a_{np}$ (fm)	5.412	5.417	5.419(7)

TABLE II: Deuteron binding energy  $B_d$  (in MeV) and  $D$ -state probability (in %),  $nn$  and singlet and triplet  $np$  scattering lengths (in fm), calculated with the two-nucleon potentials AV18 and N3LO. The experimental results are from Ref. [39].

Finally, we define

$$\bar{\Psi}^{LSJJ_z} = \sum_{L'S'} [\delta_{L,L'} \delta_{S,S'} - i \mathcal{R}_{LS,L'S'}^J(p)]^{-1} \Psi^{L'S'JJ_z}, \quad (3.14)$$

so that  $\bar{\Psi}^{LSJJ_z}$  has unit flux. The function  $\bar{\Psi}^{LSJJ_z}$  enters in Eq. (2.12) and in the expression for differential muon capture rate on deuteron.

	AV18/UIX	N3LO/N2LO	Exp.
$B_{^3\text{H}}$ (MeV)	8.479	8.474	8.482
$B_{^3\text{He}}$ (MeV)	7.750	7.733	7.718
$^2a_{nd}$ (fm)	0.590	0.675	0.645(3)(7)
$^4a_{nd}$ (fm)	6.343	6.342	6.35(2)

TABLE III: Triton and  $^3\text{He}$  binding energies  $B_{^3\text{H}}$  and  $B_{^3\text{He}}$  (in MeV), and  $nd$  doublet and quartet scattering lengths (in fm), calculated with the two- and three-nucleon potentials AV18/UIX and N3LO/N2LO. The experimental results are from Ref. [35].

#### IV. WEAK TRANSITION OPERATOR

The nuclear weak charge and current operators consist of polar- and axial-vector components. In the present work, we consider two different models, both of which have been used in studies of weak  $pp$  and  $hep$  capture reactions in the energy regime relevant to astrophysics [20–22]. The first model has been developed within the so-called “Standard Nuclear Physics Approach” (SNPA) and has been applied also to study weak transitions for  $A = 6$  and 7 nuclei [48], and magnetic moments and  $M1$  widths of nuclei with  $A \leq 7$  [49, 50]. It will be discussed in Sec. IV A. In the second model, the nuclear weak transition operators have been derived in heavy-baryon chiral perturbation theory (HBChPT), carrying out the expansion up to next-to-next-to-next-to leading order (N3LO) [22, 51]. This same model has been updated and most recently used in the electromagnetic sector to study the three-nucleon magnetic moments and

$np$  and  $nd$  radiative capture reactions in Ref. [42]. We review it in Sec. IV B.

##### A. The “Standard Nuclear Physics Approach”

The one-body axial charge and current operators have the standard expressions [21] obtained from the nonrelativistic reduction of the covariant single-nucleon current, and include terms proportional to  $1/m^2$ ,  $m$  being the nucleon mass. The induced pseudoscalar contributions are retained both in the axial current and charge operators, and are given by

$$\rho_{i,PS}^{(1)}(\mathbf{q}; A) = -\frac{g_{PS}(q_\sigma^2)}{2m m_\mu} \tau_{i,-} (m_\mu - E_\nu) \times (\boldsymbol{\sigma}_i \cdot \mathbf{q}) e^{i\mathbf{q} \cdot \mathbf{r}_i}, \quad (4.1)$$

$$\mathbf{j}_{i,PS}^{(1)}(\mathbf{q}; A) = -\frac{g_{PS}(q_\sigma^2)}{2m m_\mu} \tau_{i,-} \mathbf{q} (\boldsymbol{\sigma}_i \cdot \mathbf{q}) e^{i\mathbf{q} \cdot \mathbf{r}_i}, \quad (4.2)$$

where

$$\tau_{i,-} = (\tau_{i,x} - i\tau_{i,y})/2, \quad (4.3)$$

and  $\mathbf{q}$  is the three-momentum transfer,  $m_\mu$  the muon mass,  $E_\nu$  the neutrino energy,  $q_\sigma^2$  the squared four-momentum transfer. Note that, since in the present case  $\mathbf{q}$  is not negligible ( $q \simeq m_\mu$ ), axial and induced pseudoscalar form factors need be included. In the notation of Ref. [34], they are taken as

$$g_A(q_\sigma^2) = \frac{g_A}{(1 + q_\sigma^2/\Lambda_A^2)^2}, \quad (4.4)$$

$$g_{PS}(q_\sigma^2) = -\frac{2m_\mu m}{m_\pi^2 + q_\sigma^2} g_A(q_\sigma^2). \quad (4.5)$$

For the axial-vector coupling constant  $g_A$ , two values have been adopted in this study: the first one,  $g_A=1.2654(42)$ , is taken from Ref. [52], and has been used widely in studies of weak processes [21, 22, 34, 48]. The second one,  $g_A=1.2695(29)$ , is the latest determination quoted by the Particle Data Group (PDG) [53]. The two values for  $g_A$  are consistent with each other. In order to compare with the results of the aforementioned studies, we have adopted the earlier determination for  $g_A$ . On the other hand, to estimate the theoretical uncertainty arising from this source, the calculation has been carried out also using  $g_A=1.2695(29)$  in one specific case. As it will be shown below, the central value and the theoretical uncertainties of the considered observables are comparable in both cases.

The value for the cutoff mass  $\Lambda_A$  used in this work is 1 GeV/ $c^2$ , as in Ref. [34]. It is obtained from an analysis of pion electroproduction data [54] and measurements of the reaction  $\nu_\mu + p \rightarrow n + \mu^+$  [55]. Since here  $q_\sigma^2 \ll \Lambda_A^2$ , an uncertainty of few % on  $\Lambda_A$  is expected to affect  $g_A(q_\sigma^2)$  at the percent level. The  $q_\sigma^2$ -dependence of  $g_{PS}$  is obtained in accordance with the partially-conserved-axial-current (PCAC) hypothesis, by assuming pion-pole

dominance and the Goldberger-Treiman relation [43, 56]. In Eq. (4.5),  $m_\pi$  is the pion mass.

The two-body weak axial-charge operator includes a pion-range term, which follows from soft-pion theorem and current algebra arguments [57, 58], and short-range terms, associated with scalar- and vector-meson exchanges. The latter are obtained consistently with the two-nucleon interaction model, following a procedure [59] similar to that used to derive the corresponding weak vector-current operators [21]. The two-body axial charge operator due to  $N$ -to- $\Delta$ -transition has also been included [21, 34], although its contribution is found to be very small.

The two-body axial current operators can be divided in two classes: the operators of the first class are derived from  $\pi$ - and  $\rho$ -meson exchanges and the  $\rho\pi$ -transition mechanism. These mesonic operators, first obtained in a systematic way in Ref. [60], give rather small contributions [21]. The operators in the second class are those that give the dominant two-body contributions, and are due to  $\Delta$ -isobar excitation [20, 21]. We review them here briefly. The  $N$ -to- $\Delta$ -transition axial current is written as (in the notation of Ref. [21])

$$\mathbf{j}_i^{(1)}(\mathbf{q}; N \rightarrow \Delta, A) = - \left[ g_A^*(q_\sigma^2) \mathbf{S}_i + \frac{g_{PS}^*(q_\sigma^2)}{2m m_\mu} \mathbf{q}(\mathbf{S}_i \cdot \mathbf{q}) \right] \times e^{i\mathbf{q} \cdot \mathbf{r}_i} T_{i,\pm}, \quad (4.6)$$

where  $\mathbf{S}_i$  and  $\mathbf{T}_i$  are spin- and isospin-transition operators, which convert a nucleon into a  $\Delta$ -isobar. The induced pseudoscalar contribution has been obtained from a non-relativistic reduction of the covariant  $N$ -to- $\Delta$ -transition axial current [56].

The axial and pseudoscalar form factors  $g_A^*$  and  $g_{PS}^*$  are parameterized as

$$\begin{aligned} g_A^*(q_\sigma^2) &= R_A g_A(q_\sigma^2), \\ g_{PS}^*(q_\sigma^2) &= -\frac{2m_\mu m}{m_\pi^2 + q_\sigma^2} g_A^*(q_\sigma^2), \end{aligned} \quad (4.7)$$

with  $g_A(q_\sigma^2)$  given in Eq. (4.4). The parameter  $R_A$  is adjusted to reproduce the experimental value of the Gamow-Teller matrix element in tritium  $\beta$ -decay ( $\text{GT}^{\text{EXP}}$ ), while the  $q_\sigma^2$ -dependence of  $g_{PS}^*$  is again obtained by assuming pion-pole dominance and PCAC [43, 56]. The value for  $\text{GT}^{\text{EXP}}$ , estimated in Ref. [20], was 0.957(3). This value was determined by assuming  $g_A=1.2654(42)$ ,  $\langle \mathbf{F} \rangle^2=0.9987$ , where  $\langle \mathbf{F} \rangle$  is the reduced matrix element of the Fermi operator  $\sum_i \tau_{i,-}$ , and the triton half-life  $fT_{1/2}$  is  $(1134.6 \pm 3.1)$  s [61]. We adopt it also in the present work, except for the case in which  $g_A$  is taken from the PDG,  $g_A=1.2695(29)$ . We then extract  $\text{GT}^{\text{EXP}}=0.955(2)$ , corresponding to  $\langle \mathbf{F} \rangle^2=0.99926$  and  $fT_{1/2}=(1132.1 \pm 4.3)$  s. The new value of  $\langle \mathbf{F} \rangle^2$  differs by less than 0.1 % from the older, presumably due to the higher accuracy of the present trinucleon wave functions. The new value of  $fT_{1/2}$  has been obtained by averaging the previous value of  $fT_{1/2}$  with the new

one of Ref. [62],  $(1129.6 \pm 3)$  s, and summing the errors in quadrature. The values for  $R_A$  determined in the present study using trinucleon wave functions corresponding to the AV18/UIX are  $R_A=1.21(9)$ , when  $\text{GT}^{\text{EXP}}=0.957(3)$  and  $g_A=1.2654(42)$ , and  $R_A=1.13(6)$ , when  $\text{GT}^{\text{EXP}}=0.955(2)$  and  $g_A=1.2695(29)$ . The experimental error on  $\text{GT}^{\text{EXP}}$  is responsible for the 5–8 % uncertainty in  $R_A$ .

It is important to note that the value of  $R_A$  depends on how the  $\Delta$ -isobar degrees of freedom are treated. In the present work, as in Ref. [34], the two-body  $\Delta$ -excitation axial operator is derived in the static  $\Delta$  approximation, using first-order perturbation theory (PT). This approach is considerably simpler than that adopted in Ref. [21], where the  $\Delta$  degrees of freedom were treated non-perturbatively, within the so-called transition-correlation operator (TCO) approach, by retaining them explicitly in the nuclear wave functions [63]. The results for  $R_A$  obtained within the two schemes differ by more than a factor of 2 [21]. However, the results for the observables calculated consistently within the two different approaches are typically within 1 % of each other. Finally, because of the procedure adopted to determine  $R_A$ , the coupling constant  $g_A^*$  of Eq. (4.7) cannot be naively interpreted as the  $N\Delta$  axial coupling constant. The excitation of additional resonances and their associated contributions will contaminate the value of  $g_A^*$ .

The weak vector charge and current operators are constructed from the isovector part of the electromagnetic current, in accordance with the conserved-vector-current (CVC) hypothesis. The weak charge operator includes the non-relativistic one-body term and the relativistic spin-orbit and Darwin-Foldy contributions, and is obtained from the corresponding isovector electromagnetic operator, as listed in Ref. [64], by replacing

$$\tau_{i,z}/2 \rightarrow \tau_{i,-}. \quad (4.8)$$

Two-body contributions, arising from  $\pi$ - and  $\rho$ -meson exchange mechanisms, are also included. Their expressions are listed in Ref. [64], with the substitution

$$(\boldsymbol{\tau}_i \times \boldsymbol{\tau}_j)_z \rightarrow (\boldsymbol{\tau}_i \times \boldsymbol{\tau}_j)_-, \quad (4.9)$$

and

$$(\boldsymbol{\tau}_i \times \boldsymbol{\tau}_j)_- = (\boldsymbol{\tau}_i \times \boldsymbol{\tau}_j)_x - i(\boldsymbol{\tau}_i \times \boldsymbol{\tau}_j)_y. \quad (4.10)$$

Electromagnetic form factors are also included, and available parametrizations for them all provide excellent fits of the experimental data at the low momentum transfer of interest here.

The weak vector current operator retains the one-body operator, two-body “model-independent” (MI) and “model-dependent” (MD) terms, and three-body terms. The MI two-body currents are obtained from the two-nucleon interaction, and by construction satisfy current conservation with it. In the present work, we include the leading two-body “ $\pi$ -like” and “ $\rho$ -like” operators, obtained from the isospin-dependent central, spin-spin and



tensor nucleon-nucleon interactions. On the other hand, we have neglected the additional two-body currents arising from non-static (momentum-dependent) interactions, since these currents are short-ranged, and numerically far less important than those considered here [49]. The MD currents are purely transverse, and therefore cannot be directly linked to the underlying two-nucleon interaction. The present calculation includes the isovector currents associated with the  $\omega\pi\gamma$  transition mechanism [64], and the excitation of  $\Delta$  isobars. The former contributions are numerically negligible, while the latter are important in order to reproduce the three-nucleon magnetic moments and elastic form factors [49]. The contributions of the (MD)  $\Delta$ -isobar currents have been calculated in this case with the TCO method [63], and explicit expressions for these are listed in Ref. [65]. Again, the substitution of Eq. (4.10) is used.

A three-nucleon interaction requires a corresponding three-body current. The latter was first derived in Ref. [49] from a three-nucleon interaction consisting of a dominant two-pion-exchange component, such as the UIX model adopted in the present work. The charge-changing three-body (weak vector) current is obtained applying CVC to the operators listed in Ref. [49], i.e.

$$\left[ \frac{1}{2}(\tau_{i,a} + \tau_{j,a} + \tau_{k,a}), \mathbf{j}_{ijk,z}^{(3)}(\mathbf{q}; \gamma) \right] = i \epsilon_{azb} \mathbf{j}_{ijk,b}^{(3)}(\mathbf{q}; V), \quad (4.11)$$

where  $\mathbf{j}_{ijk,z}^{(3)}(\mathbf{q}; \gamma)$  are the isovector three-body electromagnetic currents, and  $a, b = x, y, z$  are isospin Cartesian components.

We conclude by emphasizing that the model for the weak transition operator is the same as that of Ref. [34], but for two differences relative to its vector component: (i) the MD two-body currents due to  $\Delta$ -isobar degrees of freedom are treated non perturbatively with the TCO method, rather than in first order PT, and (ii) three-body terms are also included – they were neglected in Ref. [34]. As shown in Table IV, the present model for the electromagnetic current provides an excellent description of the trinucleon magnetic moments, in particular of their isovector contribution, to better than 1 % (row labeled with “FULL”). This gives us confidence in the accuracy of the corresponding weak vector currents. We also note that: (i) three-body contributions are important to achieve this level of agreement between theory and experiment; (ii) the results obtained with the model of Ref. [34], labeled by “MD/ $\Delta$ -PT”, are at variance with data at the 3 % level; (iii) the difference between the present “FULL” results and those of Ref. [49] can be traced back to the fact that here we have used slightly more accurate wave functions, with a careful treatment of  $T = 3/2$  components. However, we should note that, in contrast to Ref. [49], MI two-body contributions arising

from non-static components of the two-nucleon interaction have been ignored. They amount to a negligible 0.1 % correction.

	${}^3\text{H}$	${}^3\text{He}$
IA	2.5745	-1.7634
MI	2.8954	-2.0790
MD/ $\Delta$ -PT	3.0260	-2.2068
MD/ $\Delta$ -TCO	2.9337	-2.1079
FULL	2.9525	-2.1299
Ref. [49]	2.953	-2.125
Exp.	2.9790	-2.1276

TABLE IV: Triton and  ${}^3\text{He}$  magnetic moments, in nuclear magnetons, calculated with the AV18/UIX Hamiltonian model and compared with the experimental data. The results labeled “IA” are obtained with single-nucleon current, while those labeled “MI” are obtained by including in addition the model-independent two-body contributions. The results labeled “MD/ $\Delta$ -PT” and “MD/ $\Delta$ -TCO” include also the model-dependent contributions, with the  $\Delta$ -isobar degrees of freedom treated in perturbation theory or within the TCO approach, respectively. Lastly, the results labeled “FULL” retain three-body contributions. Also shown are the results of Ref. [49].

## B. The chiral effective field theory approach

The  $\chi\text{EFT}$  weak transition operator is taken from Refs. [22] and [42], where it was derived in covariant perturbation theory based on the heavy-baryon formulation of chiral Lagrangians by retaining corrections up to N3LO. It was recently used in Ref. [66] to study  $M1$  electromagnetic transitions. We review its main features here.

The vector and axial-vector one-body operators are the same as those obtained within the SNPA, and described in Sec. IV A. These one-body operators are also listed in Eq. (17) of Ref. [22], except that we also include corrections in the vector current, which arise when the non-relativistic reduction is carried out to next-to-leading order (proportional to  $1/m^3$ ). The resulting operator is given (in momentum space) by

$$\mathbf{j}_i^{(1)}(\mathbf{q}; V) = \mathbf{j}_i^{(1)NR}(\mathbf{q}; V) + \mathbf{j}_i^{(1)RC}(\mathbf{q}; V), \quad (4.12)$$

where  $\mathbf{j}_i^{(1)NR}(\mathbf{q}; V)$  is the standard leading order term

$$\mathbf{j}_i^{(1)NR}(\mathbf{q}; V) = \frac{1}{m} \tau_{i,-} \left[ G_E^V(q_\sigma^2) \mathbf{k} + i G_M^V(q_\sigma^2) \boldsymbol{\sigma}_i \times \mathbf{q} \right], \quad (4.13)$$

and  $\mathbf{j}_i^{(1)RC}(\mathbf{q}; V)$  is

$$\mathbf{j}_i^{(1)RC}(\mathbf{q}; V) = -\frac{1}{4m^3}\tau_{i,-}\left[G_E^V(q_\sigma^2)\mathbf{k}^2(2\mathbf{k} + i\boldsymbol{\sigma}_i \times \mathbf{q}) + i[G_M^V(q_\sigma^2) - G_E^V(q_\sigma^2)](2\mathbf{k} \cdot \mathbf{q}\boldsymbol{\sigma}_i \times \mathbf{k} + \mathbf{k} \times \mathbf{q}\boldsymbol{\sigma}_i \cdot \mathbf{k})\right]. \quad (4.14)$$

In the above expressions,  $\mathbf{k} = (\mathbf{p}'_i + \mathbf{p}_i)/2$ ,  $\mathbf{q} = \mathbf{p}'_i - \mathbf{p}_i$ ,  $\mathbf{p}'_i$  and  $\mathbf{p}_i$  being the momenta of the outgoing and ingoing nucleons, respectively, and  $G_E^V(q_\sigma^2)$  and  $G_M^V(q_\sigma^2)$  denote the isovector combinations of the nucleon electric and magnetic form factors [64]. Note that Eqs. (4.12)–(4.14) can also be obtained from Eq. (11) of Ref. [42], with the substitution (4.8) required by CVC.

The axial two-body charge and currents are from Ref. [22]. In particular, the axial charge operator is that derived originally in Ref. [57]. In the SNPA, additional contributions are considered, which, in a  $\chi$ EFT context, are expected to appear at higher orders. The two-body axial current operator consists of two contributions: a one-pion exchange term and a (non-derivative) two-nucleon contact-term. The explicit expressions for these terms can be found in Ref. [22]. While the coupling constants which appear in the one-pion exchange term are fixed by  $\pi N$  data, the low-energy constant  $d_R$ , determining the strength of the contact-term, has been fixed by reproducing  $\text{GT}^{\text{EXP}}$ . The value  $g_A=1.2654(42)$  has been used. The values for  $d_R$  are presented in Table V and discussed below.

The two-body vector currents are decomposed into four terms [42]: the soft-one-pion-exchange ( $1\pi$ ) term, vertex corrections to the one-pion exchange ( $1\pi C$ ), the two-pion exchange ( $2\pi$ ), and a contact-term contribution. Their explicit expressions can be found in Eqs. (12)–(18) of Ref. [42], with the replacements (4.3) and (4.10) in the isospin operators. All the  $1\pi$ ,  $1\pi C$  and  $2\pi$  contributions contain low-energy constants estimated in Ref. [67], using resonance saturation arguments. The contact-term electromagnetic contribution is given by

$$\begin{aligned} \mathbf{j}_{ij}^{(2)CT}(\mathbf{q}; \gamma) = & -\frac{i}{2m} e^{i\mathbf{q}\cdot\mathbf{R}} \mathbf{q} \times [g_{4S}(\boldsymbol{\sigma}_i + \boldsymbol{\sigma}_j) \\ & + g_{4V}(\boldsymbol{\tau}_i \times \boldsymbol{\tau}_j)_z \boldsymbol{\sigma}_i \times \boldsymbol{\sigma}_j] \delta_\Lambda(r). \end{aligned} \quad (4.15)$$

The function  $\delta_\Lambda(r)$ , as well as the Yukawa functions which appear in the  $1\pi$ ,  $1\pi C$  and  $2\pi$  operators and in the two-body axial current terms, are obtained by performing the Fourier transform from momentum- to coordinate-space with a Gaussian regulator characterized by a cut-off  $\Lambda$ . This cutoff determines the momentum scale below which these EFT currents are expected to be valid, i.e.,  $\Lambda=500\text{--}800$  MeV [22]. The explicit expression of  $\delta_\Lambda(r)$  in Eq. (4.15) is

$$\delta_\Lambda(r) = \int \frac{d\mathbf{k}^3}{(2\pi)^3} e^{-k^2/\Lambda^2} e^{i\mathbf{k}\cdot\mathbf{r}}. \quad (4.16)$$

The coefficients  $g_{4S}$  and  $g_{4V}$  of Eq. (4.15) are fixed to reproduce the experimental values of triton and  $^3\text{He}$

magnetic moments, for each nuclear interaction and cut-off value. This procedure is similar to that used to fix the strength  $d_R$  of the contact-term in the two-body axial current discussed above. The results are presented in Table V. A few comments are in order: (i) while values of both  $g_{4S}$  and  $g_{4V}$  are presented, only  $g_{4V}$  is relevant in the present work, since CVC relates the isovector electromagnetic current to the weak vector current. (ii) The uncertainty on  $g_{4S}$  and  $g_{4V}$  is not due to the experimental errors on the triton and  $^3\text{He}$  magnetic moments, which are in fact negligible, but rather to numerics. We have used a random walk consisting of 1.6 million configurations, in order to reduce the numerical uncertainty on  $\Delta\mu$ , the difference between the experimental magnetic moments and the result obtained without the contact contributions, to less than 1 %. In contrast, the experimental error on  $\text{GT}^{\text{EXP}}$  is primarily responsible for the uncertainty in  $d_R$ . (iii) The values reported for  $d_R$  are different, but consistent within the error, with those listed in Table II of Ref. [22]. This is due to differences between the present  $^3\text{H}$  and  $^3\text{He}$  wave functions and those of Ref. [22] – we have already commented on this in the previous section. (iv) The  $g_{4S}$  and  $g_{4V}$  values are rather different from those listed in Ref. [66]. We observe that  $g_{4S}$  and  $g_{4V}$  are fixed by fitting very small quantities. In the AV18/UIX case with  $\Lambda = 600$  MeV, for instance, the value  $\Delta\mu$  is 0.0461(4) for triton, and  $-0.0211(4)$  for  $^3\text{He}$ , where the uncertainties are statistical errors due to the Monte Carlo integrations. Consequently, the resulting values will be sensitive to several factors, including numerics. However, it is worthwhile pointing out that the isovector contact contribution to the muon capture rates under consideration turns out to be negligible. Finally, we should point out that the present  $\chi$ EFT model for the weak vector current operator differs in some of its two-pion exchange parts from that obtained in time-ordered perturbation theory by some of the present authors in Ref. [68]. The origins of these differences have been discussed in Refs. [68, 69]. However, for consistency with the calculations of the  $pp$  and  $hep$  reactions of Ref. [22], we have chosen to use the  $\chi$ EFT model illustrated above. We do not expect these differences to be numerically significant for the processes under consideration.

## V. RESULTS

The results for the total rates of muon capture on deuteron and  $^3\text{He}$  are presented in the following two subsections.

	$\Lambda$ (MeV)	$g_{4S}$	$g_{4V}$	$d_R$
AV18/UIX	500	0.69(1)	2.065(6)	0.97(7)
	600	0.55(1)	0.793(6)	1.75(8)
	800	0.25(2)	-1.07(1)	3.89(10)
N3LO/N2LO	600	0.11(1)	3.124(6)	1.00(9)

TABLE V: The LECs  $g_{4S}$  and  $g_{4V}$  associated with the isoscalar and isovector contact terms in the electromagnetic current (see Eq. (4.15)), and the LEC  $d_R$  of the two-body axial-current contact term, calculated for three values of the cutoff  $\Lambda$  with triton and  $^3\text{He}$  wave functions obtained from the AV18/UIX model. For  $\Lambda = 600$  MeV, also the N3LO/N2LO model is also used.

SNPA (AV18)	$^1S_0$	$^3P_0$	$^3P_1$	$^3P_2$	$^1D_2$	$^3F_2$	Total
$g_A=1.2654(42)$	246.6(7)	20.1	46.7	71.6	4.5	0.9	390.4(7)
$g_A=1.2695(29)$	246.8(5)	20.1	46.8	71.8	4.5	0.9	390.9(7)
EFT* (AV18)	$^1S_0$	$^3P_0$	$^3P_1$	$^3P_2$	$^1D_2$	$^3F_2$	Total
$\Lambda = 500$ MeV	250.0(8)	19.9	46.2	71.2	4.5	0.9	392.7(8)
$\Lambda = 600$ MeV	250.0(8)	19.8	46.3	71.1	4.5	0.9	392.6(8)
$\Lambda = 800$ MeV	249.7(7)	19.8	46.4	71.1	4.5	0.9	392.4(7)
EFT* (N3LO)	$^1S_0$	$^3P_0$	$^3P_1$	$^3P_2$	$^1D_2$	$^3F_2$	Total
$\Lambda = 600$ MeV	250.5(7)	19.9	46.4	71.5	4.4	0.9	393.6(7)

TABLE VI: Total rate for muon capture on deuteron, in the doublet initial hyperfine state, in  $\text{s}^{-1}$ . The different partial wave contributions are indicated. The numbers among parentheses indicate the theoretical uncertainty arising from the adopted fitting procedures, as explained in Sec. IV. Such uncertainty is not indicated when less than  $0.1 \text{ s}^{-1}$ . The label “SNPA” indicates that the results have been obtained using the model for the weak transition operator of Sec. IV A, while the label “EFT\*” indicates that the model of Sec. IV B is used. The AV18 and N3LO interactions have been used to calculate the deuteron and  $nn$  wave functions.

### A. Muon capture on deuteron

In a partial wave expansion of the final  $nn$  state, all channels with total angular momentum  $J \leq 2$  and relative orbital angular momentum  $L \leq 3$  have been included, i.e.,  $^1S_0$ ,  $^3P_0$ ,  $^3P_1$ ,  $^3P_2$ ,  $^1D_2$  and  $^3F_2$ . Partial waves of higher order contribute less  $\simeq 0.5 \%$  to the rate. Indeed, the  $^3F_2$  contribution turns out to be already below this level.

We present in Table VI the results for the total capture rate in the doublet hyperfine state. Both models for the nuclear weak transition operator presented in Sec. IV A and Sec. IV B have been used, labeled SNPA and EFT\*, respectively. The nuclear wave functions have been calculated with the AV18 [23] or the N3LO [39] two-nucleon interaction. The label EFT\* is used to denote the results of calculations in which the matrix elements of  $\chi\text{EFT}$  weak operators are evaluated between wave functions corresponding to both conventional and chiral po-

tentials. The first approach (based on a conventional potential) is often referred to in the literature as the “hybrid” approach. The second, using chiral potentials and currents, is in principle a full-fledged  $\chi\text{EFT}$  calculation, except that these potentials and currents have not (yet) been derived consistently at the same order in the low-momentum scale. For this reason, we characterize the corresponding results with the EFT\* label.

Within each Hamiltonian model, the parameters present in the SNPA and EFT\* axial current models have been fitted to reproduce  $\text{GT}^{\text{EXP}}$  in tritium  $\beta$ -decay, as discussed in Sec. IV. Furthermore, the LECs in the EFT\* weak vector current have been fitted to reproduce the  $A = 3$  magnetic moments. The three-nucleon wave functions have been generated, in this fitting procedure, from two- and three-nucleon interactions, either AV18 and UIX [36], or N3LO and N2LO [40]. Inspection of the table shows that the  $^1S_0$  contribution is the leading one, but  $L \geq 1$  contributions are significant and account for  $\sim 37 \%$  of the total rate. By comparison between the first and second row of the table, we conclude that there is no difference in the results, within uncertainties, when the older value for  $g_A$ ,  $g_A=1.2654(42)$ , or the most recent one,  $g_A=1.2695(29)$ , is used. This reflects the fact that the factor  $R_A$ , see Sec. IV A, has been constrained by  $\text{GT}^{\text{EXP}}$  in both cases. The model dependence due to interactions, currents, and the cutoff  $\Lambda$  (present in the  $\chi\text{EFT}$  version of these currents) is at the 1 % level in the total rate, and hence very weak. It is a bit larger, 2 %, in the  $^1S_0$  channel, for which two-body current contributions are larger, see Tables VII and VIII below. In conclusion, a total capture rate in the range

$$\Gamma^D = (389.7 - 394.3) \text{ s}^{-1}, \quad (5.1)$$

can be conservatively ascribed to reaction (1.1). This result is in agreement with the measurements of Refs. [5, 6, 8], but not with that of Ref. [7]. The differences with the theoretical results of Refs. [16–18] are also very small. In particular, the authors of Ref. [18] find  $\Gamma^D(^1S_0) = 245 \text{ s}^{-1}$ , in contrast to  $\Gamma^D(^1S_0) = 250 \text{ s}^{-1}$  reported here. We have explicitly verified that this difference is mainly due to the inclusion in the present work of mesonic two-body contributions in the weak vector current beyond the soft one-pion exchange term discussed in Sec. IV B. On the other hand, the results of Refs. [15, 19] are significantly larger than those listed here, presumably because these authors have not constrained their weak current to reproduce  $\text{GT}^{\text{EXP}}$  and the isovector magnetic moment of the trinucleons. We observe that our approach also provides a value for muon capture on  $^3\text{He}$  in excellent agreement with the experimental datum.

For future reference, we show in Fig. 1 the differential capture rate  $d\Gamma^D/dp$ , defined in Eq. (2.21), as function of the  $nn$  relative momentum  $p$ , calculated with the SNPA (AV18) model. Integrating each partial wave contribution leads to the values listed in the first row of Table VI.

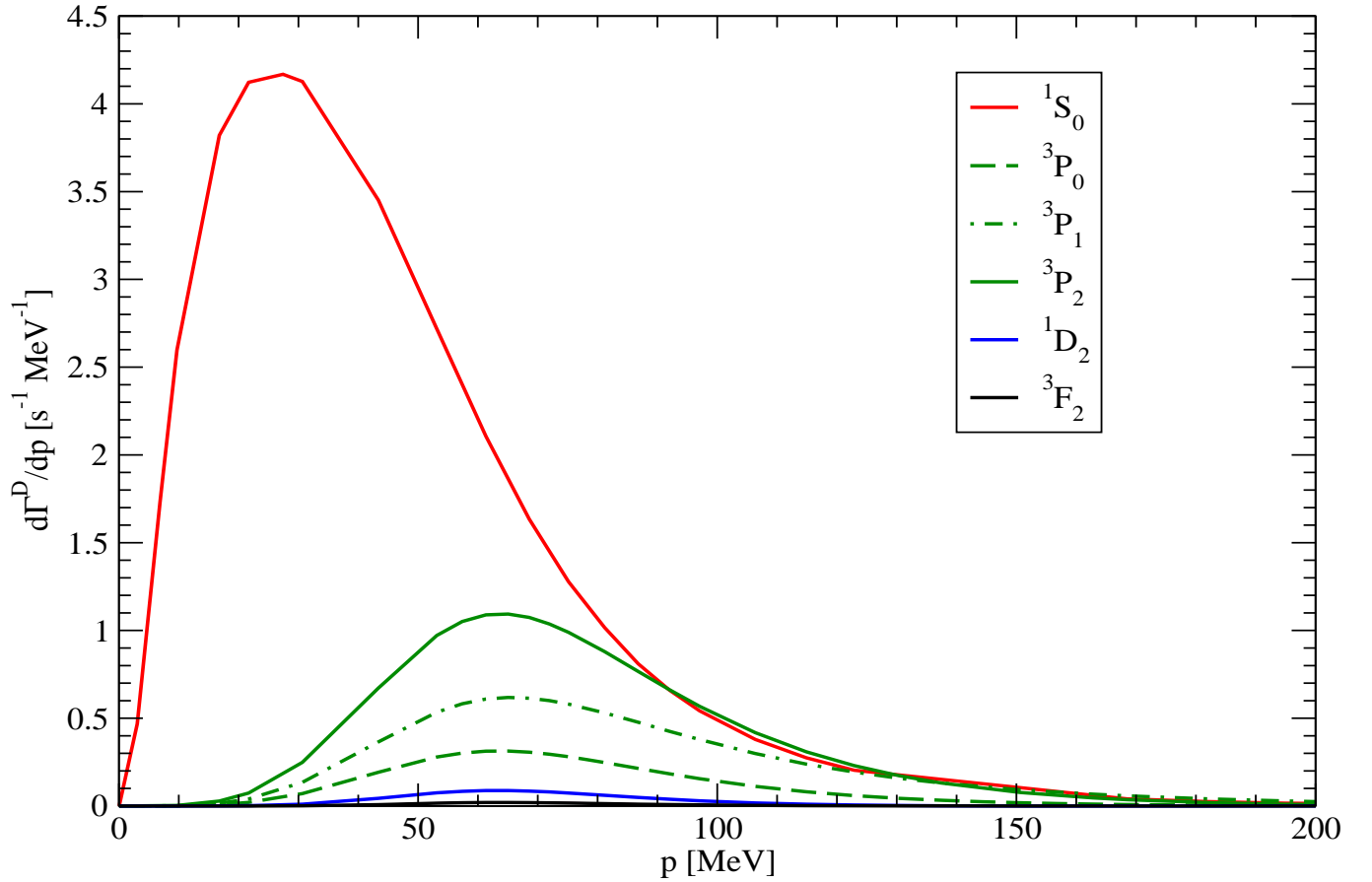


FIG. 1: (Color online) Differential capture rate  $d\Gamma^D/dp$ , defined in Eq. (2.21), as function of the  $nn$  relative momentum  $p$  in MeV. The calculation is performed with the SNPA (AV18) model.

The cumulative contributions to the leading  $^1S_0$  and  $^3P_2$  capture rates of various terms in the nuclear current operator are given in Table VII for the SNPA and VIII for the EFT\*. Table VII shows that: (i) the (one-body) induced pseudoscalar contribution is significant, as expected, and reduces the rate of  $\sim 20\%$  ( $\sim 13\%$ ) in  $^1S_0$  ( $^3P_2$ ) capture; (ii) the mesonic contributions are very small; (iii) the  $\Delta$ -isobar contributions are significant only in  $S$ -wave capture, and differences in the vector two-body current originating from treating the  $\Delta$ -isobar degrees of freedom either perturbatively or within the TCO approach are negligible; (iv) the  $\Delta$ -isobar induced pseudoscalar axial current contribution of Eqs. (4.6) and (4.7) is of the order of  $1\text{ s}^{-1}$  for  $^1S_0$  capture.

From inspection of Table VIII, we can conclude that: (i) the one-body contributions (labeled “IA+RC” and “PS”) are slightly different from those reported in the SNPA. While the EFT\* one-body axial charge and current, and vector charge, operators are the same as in the SNPA, the EFT\* one-body vector current includes

the relativistic corrections of Eq. (4.14), ignored in the SNPA. On the other hand, the differences between SNPA and EFT\* one-body contributions remain well below the 1 % level, and therefore within the theoretical uncertainty. However, it would be interesting to study the contributions of these relativistic corrections to the many electromagnetic observables analyzed within the SNPA over the years [49, 50]. A first step in this direction has been done in Ref. [70]. (ii) The  $\Lambda$  dependence is very weak, well below the 1 % level. (iii) The  $^3P_2$  term does not show any  $\Lambda$  dependence nor any sensitivity to the  $d_R$  and  $g_{4V}$  fitting procedure. This is easily understood by observing that the contact terms in the vector and axial currents are proportional to  $(\boldsymbol{\tau}_i \times \boldsymbol{\tau}_j)_-(\boldsymbol{\sigma}_i \times \boldsymbol{\sigma}_j)$  (see Ref. [22] and Eq. (4.15)), whose matrix elements vanish when calculated between the deuteron state and  $^3P_J$   $nn$  states.

By comparison of the results listed in Tables VII and VIII, we observe that the main source for the 2 % theoretical uncertainty in the  $^1S_0$  channel quoted above is the  $\Delta$ -isobar induced pseudoscalar contribution: were it to be neglected, the SNPA and EFT\*  $^1S_0$  results would

	$^1S_0$	$^3P_2$
IA+RC	293.0	82.6
PS	233.2	71.6
mesonic	237.5	71.4
$\Delta$ -PT(A-w/o PS)+ $\Delta$ -PT(V)	248.3(8)	71.6
$\Delta$ -PT(A-w/o PS)+ $\Delta$ -TCO(V)	247.7(8)	71.6
$\Delta$ -PT(A-w PS)+ $\Delta$ -TCO(V)	246.6(7)	71.6

TABLE VII: Cumulative contributions to the total rate for muon capture on deuteron in  $s^{-1}$ , when the model of Sec. IV A is used for the weak transition operator. The deuteron and  $nn$  wave functions are calculated using the AV18 interaction. Only the  $^1S_0$  and  $^3P_2$  partial waves are considered, since they give the leading contributions. The labels “IA+RC”, “PS”, and “mesonic” indicate the results obtained by retaining the impulse approximation plus relativistic corrections, the induced pseudoscalar, and the purely mesonic contributions. The label “ $\Delta$ -PT(A-w/o PS)” is used to indicate that the axial charge and current contributions due to  $\Delta$ -isobars are retained perturbatively, but the induced pseudoscalar contribution in the one-body  $\Delta$ -current is not included, while the label “ $\Delta$ -PT(A-w PS)” is used when the  $N$ -to- $\Delta$  induced pseudoscalar contribution is also included. Finally, the labels “ $\Delta$ -PT(V)” and “ $\Delta$ -TCO(V)” are used when the vector current contributions due to  $\Delta$ -isobars are treated perturbatively and within the TCO scheme, respectively. The value  $g_A=1.2654(42)$  is used. The numbers in parentheses indicate the theoretical errors arising from the fitting procedure adopted for  $R_A$ . This uncertainty is not shown if less than  $0.1 s^{-1}$ .

agree at the 1 % level. We observe that the strength of the associated operator, which is only included in the SNPA calculation and plays no role in tritium  $\beta$ -decay (being proportional to the momentum transfer  $\mathbf{q}$ ), follows from PCAC and pion-dominance arguments, see Sec. IV A.

### B. Muon capture on $^3\text{He}$

We present in Table IX the results for the total capture rate  $\Gamma_0$  defined in Eq. (2.19). The theoretical uncertainties due to the fitting procedure of  $R_A$  (SNPA) or  $d_R$  and  $g_{4V}$  (EFT\*) are in parentheses. The results in the first two rows have been obtained in the SNPA, using the AV18/UIX Hamiltonian and the two available values for  $g_A$ . These results are the same, since a change in  $g_A$  is compensated by a corresponding one in  $R_A$ . The results of the next three rows have been obtained within the hybrid approach EFT\* (AV18/UIX). They show a very weak  $\Lambda$ -dependence, and are in excellent agreement with those reported in SNPA. The result in the last row is with the EFT\* (N3LO/N2LO). The EFT\* (AV18/UIX) and EFT\* (N3LO/N2LO) differ by  $8 s^{-1}$ , or less than 1 %. In view of this, we quote conservatively a total capture rate for reaction (1.2) in the range

$$\Gamma_0 = (1471 - 1497) s^{-1}, \quad (5.2)$$

	$^1S_0$	$^3P_2$
IA+RC	292.5	82.5
$\Lambda = 500 \text{ MeV}$ PS	232.7	71.6
mesonic	250.0(8)	71.2
IA+RC	292.5	82.5
$\Lambda = 600 \text{ MeV}$ PS	232.7	71.6
mesonic	250.0(8)	71.1
IA+RC	292.5	82.5
$\Lambda = 800 \text{ MeV}$ PS	232.7	71.6
mesonic	249.7(7)	71.1

TABLE VIII: Same as Table VII but with the nuclear current model of Sec. IV B. The labels “IA+RC”, “PS”, and “mesonic” indicate the results obtained by retaining the impulse approximation plus relativistic corrections, the induced pseudoscalar, and the mesonic contributions. The relativistic corrections to the one-body vector current operator include the additional terms of Eq. (4.14). The numbers in parentheses indicate the theoretical errors arising from the fitting procedure adopted for  $d_R$  and  $g_{4V}$ . This uncertainty is not shown if less than  $1 s^{-1}$ .

by keeping the lowest and upper bounds in the values of Table IX.

SNPA (AV18/UIX)	$\Gamma_0$
$g_A=1.2654(42)$	1486(8)
$g_A=1.2695(29)$	1486(5)
EFT* (AV18/UIX)	$\Gamma_0$
$\Lambda = 500 \text{ MeV}$	1487(8)
$\Lambda = 600 \text{ MeV}$	1488(9)
$\Lambda = 800 \text{ MeV}$	1488(8)
EFT* (N3LO/N2LO)	$\Gamma_0$
$\Lambda = 600 \text{ MeV}$	1480(9)
EXP.	1496(4)

TABLE IX: Total rate for muon capture on  $^3\text{He}$ , in  $s^{-1}$ . The numbers in parentheses indicate the theoretical uncertainties due to the adopted fitting procedure, see Sec. IV. The label “SNPA” (“EFT\*”) indicates that the results have been obtained using the model for the weak transition operator of Sec. IV A (Sec. IV B). The triton and  $^3\text{He}$  wave functions are obtained from the AV18/UIX and N3LO/N2LO Hamiltonians.

The contributions of the different components of the weak current and charge operators to the total rate and to the reduced matrix elements (RMEs) of the contributing multipoles are reported in Table X for SNPA and XI for EFT\*. The HH wave functions have been calculated using the AV18/UIX Hamiltonian model. In Table X,  $R_A$  has been fixed to its central value 1.21, and in Table XI we use  $\Lambda = 600 \text{ MeV}$  and consequently  $d_R = 1.75$  and  $g_{4V} = 0.793$  (see Table V). The notation in these tables

is the same as that of Tables VII and VIII of Sec. V A, with the only exception of the label “ $\Delta$ -TCO(V)”, which here indicates that the two-body  $\Delta$ -currents are treated with the TCO method, and that the three-body current, constructed consistently with the UIX three-nucleon interaction, are also included. In Table X, we observe that the induced pseudoscalar term gives a significant contribution to the  $L_1(A)$  and  $C_1(A)$  RMEs, although the latter is much smaller than  $L_1(A)$  in magnitude. The mesonic contributions to  $C_0(V)$ ,  $C_1(A)$ ,  $L_1(A)$ , and  $E_1(A)$  are small, while they provide a 15 % correction to  $M_1(V)$ , as expected (in the isovector magnetic moments of the trinucleons, these mesonic currents give a 15 % contribution relative to the one-body). Contributions due to  $\Delta$ -isobar excitations in the weak vector and axial currents are at the few % level. Finally, we note that the result for  $\Gamma_0$  is in excellent agreement with that of the earlier study of Ref. [34]. This agreement comes about because of two compensating effects: on the one hand, the  $L_1(A)$  and  $E_1(A)$  RMEs are, in magnitude, slightly larger, as consequence of the fact that the parameter  $R_A$  is slightly larger here than in Ref. [34], because of the more accurate wave functions employed. On the other hand, the  $M_1(V)$  RME corresponding to  $\Delta$ -TCO(V) is slightly smaller than calculated in Ref. [34],  $M_1(V) = 0.1355$  in Ref. [34] versus  $M_1(V) = 0.1346$ . This last value results from dividing the value listed in Table X by the factor 1.022, arising from the normalization correction of the trinucleon wave functions due to the presence of explicit  $\Delta$ -isobar degrees of freedom, i.e.,  $N_\Delta = \sqrt{\langle \Psi_{N+\Delta} | \Psi_{N+\Delta} \rangle / \langle \Psi_{N\text{only}} | \Psi_{N\text{only}} \rangle}$ , where  $\Psi_{N+\Delta}$  ( $\Psi_{N\text{only}}$ ) is the nuclear wave function with both nucleon

and  $\Delta$  (nucleon only) degrees of freedom. Indeed, the  $\Delta$ -TCO(V)  $M_1(V)$  RME should be compared with  $M_1(V)$  corresponding to  $\Delta$ -PT(V) in Table X.

In Table XI, we observe that: (i) the one-body vector current contribution to the  $M_1(V)$  RME is different than in SNPA. This is due to the presence of the additional relativistic corrections of Eq. (4.14). (ii) The mesonic contributions are significant for the  $L_1(A)$ ,  $E_1(A)$  and  $M_1(V)$  RMEs, and bring their values closer to those in the SNPA. (iii) The  $1\pi C$ ,  $2\pi$ , and contact terms in the mesonic vector current are important. If they were to be neglected, the total  $M_1(V)$  RME would be equal to 0.1201 and consequently  $\Gamma_0 = 1453 \text{ s}^{-1}$ . (iv) The results of Table XI should be compared with those of Table 2 of Ref. [37]. We find significant differences in all the RMEs, both for the one-body contribution (here labeled “PS” and in Ref. [37] “IA”) and the complete calculation. Only the results for the  $M_1(V)$  RME appear to be similar to each other, although it is unclear whether in Ref. [37] the vector  $1\pi C$ ,  $2\pi$  and contact-term contributions are included.

Finally, we observe that when the N3LO/N2LO Hamiltonian model is used,  $C_0(V)$ ,  $C_1(A)$ ,  $L_1(A)$ ,  $E_1(A)$  and  $M_1(V)$  are  $-0.3288$ ,  $0.4130 \times 10^{-2}$ ,  $-0.2773$ ,  $-0.5810$  and  $0.1329$ , respectively, when the mesonic contributions are included. Comparing these results with the AV18/UIX ones of Table XI, we see that all the RMEs are comparable at the 1 % level. This fact is reflected in the  $\sim 1$  % difference between the AV18/UIX and N3LO/N2LO results for  $\Gamma_0$ . Therefore, it does not seem possible to identify a particular source for this 1 % difference.

	$\Gamma_0$	$C_0(V)$	$C_1(A)$	$L_1(A)$	$E_1(A)$	$M_1(V)$
IA+RC	1530	-0.3287	$0.7440 \times 10^{-2}$	-0.4056	-0.5516	0.1127
PS	1316		$0.3986 \times 10^{-2}$	-0.2589		
mesonic	1385	-0.3283	$0.4024 \times 10^{-2}$	-0.2619	-0.5562	0.1315
$\Delta$ -PT(A-w/o PS)+ $\Delta$ -PT(V)	1501		$0.4287 \times 10^{-2}$	-0.2811	-0.5821	0.1370
$\Delta$ -PT(A-w/o PS)+ $\Delta$ -TCO(V)	1493					0.1376
$\Delta$ -PT(A-w PS)+ $\Delta$ -TCO(V)	1486			-0.2742		

TABLE X: Cumulative contributions to the total rate  $\Gamma_0$  for muon capture on  $^3\text{He}$ , in  $\text{s}^{-1}$ , and to the reduced matrix elements (RMEs)  $C_0(V)$ ,  $C_1(A)$ ,  $L_1(A)$ ,  $E_1(A)$  and  $M_1(V)$  (see Sec. II), when the model of Sec. IV A is used for the weak transition operator ( $R_A = 1.21$ ). The HH wave functions have been calculated using the AV18/UIX Hamiltonian. Notation is the same as in Table VII, except for “ $\Delta$ -TCO(V)”, which here is used to indicate that the  $\Delta$ -isobar contributions are treated with the TCO method, and, in addition, three-body weak vector current contributions are included. Note that  $C_0(V)$  is purely real, while the other RMEs are purely imaginary.

## VI. SUMMARY AND CONCLUSIONS

Total rates for muon capture on deuteron and  $^3\text{He}$  have been calculated within a consistent approach, based

	$\Gamma_0$	$C_0(V)$	$C_1(A)$	$L_1(A)$	$E_1(A)$	$M_1(V)$
IA+RC	1517	-0.3287	$0.7440 \times 10^{-2}$	-0.4056	-0.5516	0.1082
PS	1303		$0.3986 \times 10^{-2}$	-0.2589		
mesonic	1488		$0.3978 \times 10^{-2}$	-0.2810	-0.5833	0.1317

TABLE XI: Same as Table X but with the nuclear current model of Sec. IV B. The value for the cutoff  $\Lambda$  has been fixed to 600 MeV, and  $d_R = 1.75$  and  $g_{4V} = 0.793$ . Notation is the same as in Table VIII.

on realistic interactions and weak currents consisting of vector and axial-vector components with one- and many-body terms. Two different approaches have been used to derive these operators: the first one goes beyond the impulse approximation, by including meson-exchange current contributions and terms arising from the excitation of  $\Delta$ -isobar degrees of freedom. This approach, labeled SNPA, has been widely and successfully used in studies of electroweak processes (see for instance Refs. [20, 21, 34, 46, 49]). The second approach, labeled EFT\*, includes two-body contributions, beyond the impulse approximation, derived within a systematic  $\chi$ EFT expansion, up to N3LO. The only parameter in the SNPA nuclear weak current model is present in the axial current and is determined by fitting the experimental value for the triton half-life. In the case of the EFT\* approach, two LECs appear, one in the vector and one in the axial-vector component (note that the LEC appearing in the isoscalar electromagnetic contact term does not contribute here). They are fixed to reproduce, respectively, the  $A = 3$  isovector magnetic moment and triton half-life.

Our final results are summarized in Eqs. (5.1) and (5.2). The very accurate experimental datum of Ref. [14] for the total rate in muon capture on  $^3\text{He}$  is very well reproduced. For the muon capture on deuteron, a precise measurement should become available in the near future [9]. The dependence of the results on the input Hamiltonian model, or on the model for the nuclear transition operator, is weak, at less than 1 % level. This weak model dependence is a consequence of the procedure adopted to constrain the weak current.

We conclude by noting that (i) within the EFT\* approach, the two-body vector current operators beyond the one-pion-exchange term give significant contributions to the total rate, especially for muon capture on  $^3\text{He}$ .

These terms have been included in the study of weak processes here for the first time. However, since they are proportional to the momentum transfer, their contribution is expected to be negligible in the  $pp$  and  $hep$  reactions [22]. (ii) Some of the radiative corrections are accounted for in the present predictions for the muon rates, since the value adopted for the Fermi coupling constant  $G_V$  is that extracted from an analysis of superallowed  $\beta$ -decays [44]. The size of these corrections (roughly 2.4 % on  $G_V^2$ ) is in agreement with that calculated independently in Ref. [71] for the muon capture on hydrogen and helium. The additional radiative corrections, originating from vacuum polarization effects on the muon bound-state wave function, have also been estimated by the authors of Ref. [71]. In the case of the muon capture on  $^3\text{He}$ , they increase the predicted rates by about 0.68%, leading to  $1496 \text{ s}^{-1}$  for the AV18/UIX model, and to  $1490 \text{ s}^{-1}$  for the EFT\*(N3LO/N2LO) model, and thus bringing them into closer agreement with experiment. (iii) The value for the induced pseudoscalar coupling used in the present study,  $g_{PS} = -8.28$  at the four-momentum transfer relevant for muon capture on  $^3\text{He}$  ( $q_\sigma^2 = 0.954m_\mu^2$ ), is consistent with that predicted by PCAC and chiral perturbation theory [72]. The agreement between the calculated and experimental muon capture rates confirms the validity of these predictions. (iv) The agreement between our final results for the muon capture rate on  $^3\text{He}$  and those of Ref. [37] confirms the tight limits obtained there on possible contributions from second class currents.

Finally, we remark that it would be interesting to extend these calculations to the processes  $\mu^- + ^3\text{He} \rightarrow n + d + \nu_\mu$  and  $\mu^- + ^4\text{He} \rightarrow n + ^3\text{H} + \nu_\mu$ , for which experimental data are also available [73, 74].

## Acknowledgments

One of the authors (R.S.) would like to thank the Physics Department of the University of Pisa, the INFN Pisa branch, and especially the Pisa group for the continuing support and warm hospitality, extended to him over the past several years.

The work of R.S. is supported by the U.S. Department of Energy, Office of Nuclear Science, under contract DE-AC05-06OR23177.

---

[1] D.F. Measday, Phys. Rep. **354**, 243 (2001).  
[2] T. Gorringer and H.W. Fearing, Rev. Mod. Phys. **76**, 31 (2004).  
[3] S. Vaintraub, N. Barnea, and D. Gazit, Phys. Rev. C **79**, 065501 (2009); E. O'Connor *et al.*, Phys. Rev. C **75**, 055803 (2007); D. Gazit and N. Barnea, Phys. Rev. Lett. **98**, 192501 (2007).  
[4] E.G. Adelberger *et al.*, arXiv:1004.2318.

[5] I.-T. Wang *et al.*, Phys. Rev. **139**, B1528 (1965).  
[6] A. Bertin *et al.*, Phys. Rev. D **8**, 3774 (1973).  
[7] G. Bardin *et al.*, Nucl. Phys. A **453**, 591 (1986).  
[8] M. Cargnelli *et al.*, *Workshop on fundamental  $\mu$  physics*, Los Alamos, 1986, LA 10714C; *Nuclear Weak Process and Nuclear Structure, Yamada Conference XXIII*, ed. M. Morita, H. Ejiri, H. Ohtsubo, and T. Sato (World Scientific, Singapore), p. 115 (1989).

- [9] V.A. Andreev *et al.* (MuSun Collaboration), <http://www.npl.illinois.edu/exp/musun>, (2007).
- [10] I.V. Falomkin *et al.*, Phys. Lett. **3**, 229 (1963).
- [11] O.A. Zaimidoroga *et al.*, Phys. Lett. **6**, 100 (1963).
- [12] L.B. Auerbach *et al.*, Phys. Rev. **138**, B127 (1965).
- [13] D.R. Clay, J.W. Keuffel, R.L. Wagner, and R.M. Edelstein, Phys. Rev. **140**, B587 (1965).
- [14] P. Ackerbauer *et al.*, Phys. Lett. B **417**, 224 (1998).
- [15] J. Adam and E. Truhlik, Nucl. Phys. A **507**, 675 (1990).
- [16] N. Tatara, Y. Kohyama, and K. Kubodera, Phys. Rev. C **42**, 1694 (1990).
- [17] M. Doi *et al.*, Nucl. Phys. A **511**, 507 (1990); Prog. Theor. Phys. **86**, 13 (1991).
- [18] S. Ando *et al.*, Phys. Lett. B **533**, 25 (2002).
- [19] P. Ricci, E. Truhlik, B. Mosconi, and J. Smejkal, Nucl. Phys. A **837**, 110 (2010).
- [20] R. Schiavilla *et al.*, Phys. Rev. C **58**, 1263 (1998).
- [21] L.E. Marcucci, R. Schiavilla, M. Viviani, A. Kievsky, and S. Rosati, Phys. Rev. Lett. **84**, 5959 (2000); L.E. Marcucci, R. Schiavilla, M. Viviani, A. Kievsky, S. Rosati, and J.F. Beacom, Phys. Rev. C **63**, 015801 (2000).
- [22] T.-S. Park *et al.*, Phys. Rev. C **67**, 055206 (2003).
- [23] R.B. Wiringa, V.G.J. Stoks, and R. Schiavilla, Phys. Rev. C **51**, 38 (1995).
- [24] V.G.J. Stoks, R.A.M. Klomp, C.P.F. Terheggen, and J.J. de Swart, Phys. Rev. C **49**, 2950 (1994).
- [25] J.-W. Chen, T. Inoue, X. Ji, and Y. Li, Phys. Rev. C **72**, 061001(R) (2005).
- [26] J.G. Congleton and H.W. Fearing, Nucl. Phys. A **552**, 534 (1992).
- [27] J.G. Congleton and E. Truhlik, Phys. Rev. C **53**, 956 (1996).
- [28] R.B. Wiringa, R.A. Smith, and T.L. Ainsworth, Phys. Rev. C **29**, 1207 (1984).
- [29] S.A. Coon *et al.*, Nucl. Phys. A **317**, 242 (1979).
- [30] E.C.Y. Ho, H.W. Fearing, and W. Schadow, Phys. Rev. C **65**, 065501 (2002).
- [31] W.N. Cottingham *et al.*, Phys. Rev. D **8**, 800 (1973).
- [32] R. Machleidt, K. Holinde, and Ch. Elster, Phys. Rep. **149**, 1 (1987); R. Machleidt, Adv. Nucl. Phys. **19**, 189 (1989).
- [33] R. Machleidt, Phys. Rev. C **63**, 024001 (2001).
- [34] L.E. Marcucci, R. Schiavilla, S. Rosati, A. Kievsky, and M. Viviani, Phys. Rev. C **66**, 054003 (2002).
- [35] A. Kievsky *et al.*, J. Phys. G: Nucl. Part. Phys. **35**, 063101 (2008).
- [36] B.S. Pudliner, V.R. Pandharipande, J. Carlson, and R.B. Wiringa, Phys. Rev. Lett. **74**, 4396 (1995).
- [37] D. Gazit, Phys. Lett. B **666**, 472 (2008).
- [38] N. Barnea, W. Leidemann, and G. Orlandini, Phys. Rev. C **61**, 054001 (2000); Nucl. Phys. A **693**, 565 (2001); N. Barnea and A. Novoselsky, Ann. Phys. (N.Y.) **256**, 192 (1997).
- [39] D.R. Entem and R. Machleidt, Phys. Rev. C **68**, 041001 (2003).
- [40] P. Navrátil, Few-Body Syst. **41**, 117 (2007).
- [41] E. Epelbaum, U.-G. Meissner, and W. Glockle, Nucl. Phys. A **747**, 362 (2005).
- [42] Y.-H. Song, R. Lazauskas, and T.-S. Park, Phys. Rev. C **79**, 064002 (2009).
- [43] J.D. Walecka, *Theoretical Nuclear and Subnuclear Physics* (Oxford University Press, New York, 1995).
- [44] J.C. Hardy *et al.*, Nucl. Phys. A **509**, 429 (1990).
- [45] M. Viviani *et al.*, Few-Body Syst. **39**, 159 (2006).
- [46] L.E. Marcucci, A. Kievsky, L. Girlanda, S. Rosati, and M. Viviani, Phys. Rev. C **80**, 034003 (2009).
- [47] W. Kohn, Phys. Rev. **74**, 1763 (1948).
- [48] R. Schiavilla and R.B. Wiringa, Phys. Rev. C **65**, 054302 (2002).
- [49] L.E. Marcucci, M. Viviani, R. Schiavilla, A. Kievsky, and S. Rosati, Phys. Rev. C **72**, 014001 (2005).
- [50] L.E. Marcucci, M. Pervin, S.C. Pieper, R. Schiavilla, and R.B. Wiringa, Phys. Rev. C **78**, 065501 (2008).
- [51] Y.-H. Song *et al.*, Phys. Lett. B **656**, 174 (2007).
- [52] E. Adelberger *et al.*, Rev. Mod. Phys. **70**, 1265 (1998).
- [53] C. Amsler *et al.* (Particle Data Group), Phys. Lett. B **667**, 1 (2008).
- [54] E. Amaldi, S. Fubini, and G. Furlan, *Electroproduction at Low Energy and Hadron Form Factors*, (Springer Tracts in Modern Physics No. 83, 1979), p.1.
- [55] T. Kitagaki *et al.*, Phys. Rev. D **28**, 436 (1983).
- [56] T.R. Hemmert, B.R. Holstein, and N.C. Mukhopadhyay, Phys. Rev. D **51**, 158 (1995).
- [57] K. Kubodera, J. Delorme, and M. Rho, Phys. Rev. Lett. **40**, 755 (1978).
- [58] I.S. Towner, Nucl. Phys. A **542**, 631 (1992).
- [59] M. Kirchbach, D.O. Riska, and K. Tsushima, Nucl. Phys. A **542**, 616 (1992).
- [60] M. Chemtob and M. Rho, Nucl. Phys. A **163**, 1 (1971).
- [61] J.J. Simpson, Phys. Rev. C **35**, 752 (1987).
- [62] Yu.A. Akulov and B.A. Mamyrin, Phys. Lett. B **610**, 45 (2005).
- [63] R. Schiavilla, R.B. Wiringa, V.R. Pandharipande, and J. Carlson, Phys. Rev. C **45**, 2628 (1992).
- [64] J. Carlson and R. Schiavilla, Rev. Mod. Phys. **70**, 743 (1998).
- [65] M. Viviani, R. Schiavilla, and A. Kievsky, Phys. Rev. C **54**, 534 (1996).
- [66] R. Lazauskas, Y.-H. Song, and T.-S. Park, arXiv:0905.3119.
- [67] T.-S. Park, D.-P. Min, and M. Rho, Phys. Rev. Lett. **74**, 4153 (1995); T.-S. Park, K. Kubodera, D.-P. Min, and M. Rho, Phys. Rev. C **58**, R637 (1998); T.-S. Park, K. Kubodera, D.-P. Min, and M. Rho, Phys. Lett. B **472**, 232 (2000).
- [68] S. Pastore *et al.*, Phys. Rev. C **80**, 034004 (2009).
- [69] S. Kölling, E. Epelbaum, H. Krebs, and U.-G. Meissner, Phys. Rev. C **80**, 045502 (2009).
- [70] L. Girlanda *et al.*, arXiv:1008.0356
- [71] A. Czarnecki, W.J. Marciano, and A. Sirlin, Phys. Rev. Lett. **99**, 032003 (2007).
- [72] S.L. Adler and Y. Dothan, Phys. Rev. **151**, 1267 (1966); N. Kaiser, Phys. Rev. C **67**, 027002 (2003); V. Bernard, N. Kaiser, and U.-G. Meissner, Phys. Rev. D **50**, 6899 (1994).
- [73] S.E. Kuhn *et al.*, Phys. Rev. C **50**, 1771 (1994).
- [74] L.B. Auerbach *et al.*, Phys. Rev. B **138**, 127 (1967); R. Bizzarri *et al.*, Nuovo Cimento **33**, 1497 (1964); M.M. Block *et al.*, Nuovo Cimento **55**, 501 (1968).